

RoadMamba: A Dual-Branch Visual State Space Model for Road Surface Classification

Tianze Wang *, Zhang Zhang *, Chao Yue, Nuoran Li, Chao Sun †

Beijing Institute of Technology
chaosun@bit.edu.cn

Abstract

Acquiring the road surface conditions in advance based on visual technologies provides effective information for the planning and control system of autonomous vehicles, thus improving the safety and driving comfort of the vehicles. Recently, the Mamba architecture based on state-space models has shown remarkable performance in visual processing tasks, benefiting from the efficient global receptive field. However, existing Mamba architectures struggle to achieve state-of-the-art visual road surface classification due to their lack of effective extraction of the local texture of the road surface. In this paper, we explore for the first time the potential of visual Mamba architectures for road surface classification task and propose a method that effectively combines local and global perception, called RoadMamba. Specifically, we utilize the Dual State Space Model (DualSSM) to effectively extract the global semantics and local texture of the road surface and decode and fuse the dual features through the Dual Attention Fusion (DAF). In addition, we propose a dual auxiliary loss to explicitly constrain dual branches, preventing the network from relying only on global semantic information from the deep large receptive field and ignoring the local texture. The proposed RoadMamba achieves the state-of-the-art performance in experiments on a large-scale road surface classification dataset containing 1 million samples.

Introduction

Autonomous vehicles (Geiger et al. 2013), (Caesar et al. 2020), (Sun et al. 2020) and intelligent transportation system (Yu et al. 2022; Zhang et al. 2025a; Yang et al. 2023; Zhang et al. 2025b) have been widely explored and developed in recent years, making vehicle safety and ride comfort become increasingly important. Accurate road surface information, including friction levels, uneven conditions and more, helps driving system control their vehicles within a safe and comfortable range. As cameras are becoming the standard for driving environment sensing, many studies (Nolte, Kister, and Maurer 2018; Leng et al. 2021; Tian et al. 2021; Dhi-man and Klette 2019; Šabanovič et al. 2020; Zhao et al. 2023; Wang, Zhang, and Sun 2025) have verified that vision-based road surface perception is one of the effective and superior methods. Specifically, it performs fine-grained classification of road surface images collected by the on-board

camera using Deep Neural Network (DNN), such as the friction level, unevenness, and material properties of the road surface. Among them, the subclasses of the three road properties are combined to model it as a classification task with 27 classes. Fine-grained road surface classification with different combinations of road attributes requires the network not only to be able to obtain accurate global semantics from the road, but also not to ignore the local nuances of the surface texture, which pose a challenge to existing image classification networks. For example, the material and friction level of the road surface are mainly obtained from the global semantics of the image, while the damage and unevenness level of the road surface are mainly recognized from some local details.

Recently, visual Mamba (Gu and Dao 2023; Zhu et al. 2024; Liu et al. 2024; Guo et al. 2024; Chen et al. 2025; Zhang et al. 2025c) based on State Space Model (SSM) has emerged as an efficient and effective backbone for constructing deep networks. This development offers a potential solution for efficient long-range modeling in road surface classification. Specifically, the discretized recursive state-space equations and the parallel scanning algorithm in Mamba can efficiently model very long-range dependencies, striking a balance between global receptive fields and computational burden compared to the standard Transformer. This implies that Mamba-based classification methods have a natural advantage in efficiently processing global pixels of road surface images and obtaining global semantics. The above desirable properties motivate us to explore the potential of visual Mamba for road surface classification.

However, existing visual Mamba architectures still face challenges when dealing with the combination of road surface properties mentioned above for road surface classification due to the lack of effective extraction of local texture. Since standard Mamba was designed to handle 1-D sequences in Natural Language Processing (NLP), it naturally faces the separation of neighboring pixels when processing 2-D signals. Although recent methods (Huang et al. 2024; Liu et al. 2024) have attempted to improve on the scanning direction and to some extent increase the modeling of local 2D dependencies, however, the local details still run the risk of being forgetting in long sequences.

To address this, we propose a method that effectively combines local and global perception, called RoadMamba.

*These authors contributed equally.

Specifically, we propose the Dual State Space Model (DualSSM) consisting of Local State Space Model (LocalSSM) branch and Global State Space Model (GlobalSSM) branch to efficiently extract the global semantics and local texture of road surfaces. To further decode and fuse the extracted global and local features, Dual Attention Fusion (DAF) is proposed. It utilizes channel attention to extract key semantic information and suppress irrelevant channels in global semantics, and retains key spatial distributions in local information through spatial attention. In addition, we propose an auxiliary loss to explicitly constrain dual branches, preventing the network from relying only on global semantic information from the deep large receptive field and ignoring the local texture.

In short, our main contributions can be summarized as follows:

- We explore for the first time the potential of visual Mamba architectures for road surface classification task and propose a framework that effectively extracts global semantics and local textures from road surface based on Dual State Space Model (DualSSM), called RoadMamba.
- In order to effectively decode and fuse the extracted global and local features, we propose the Dual Attention Fusion (DAF), which consists of lightweight global and local attention to extract key semantic and retain critical spatial distributions.
- We utilize a dual auxiliary loss to explicitly constrain dual branches, preventing the network from relying only on global semantic information from the deep large receptive field and ignoring the local texture.
- Extensive experiments on a large-scale road surface classification dataset containing 1 million samples demonstrate our RoadMamba outperforms the state-of-the-art methods.

Related Work

Road Surface Classification

The main technical route for vision-based road perception is the utilization of Deep Neural Networks (DNNs) to classify road categories or to detect road unevenness. (Roychowdhury et al. 2018) developed a classification scheme that takes into account the characteristics of the drivable surface, the sky, and the surrounding environment. (Šabanovič et al. 2020) designed a DNN-based algorithm to classify three road surfaces under dry and wet conditions. In recent years, (Zhao et al. 2023) has collected and created datasets of road surface images from real-world driving conditions that scale up to 1 million samples, labeling road images in detail with friction levels, unevenness, and material properties, which made significant advancements in the road surface classification. On this basis, RoadFormer (Wang, Zhang, and Sun 2025) achieved effective road surface classification by combining the architectures of CNN and Transformer. However,

it relies on specific combination strategies and architectural designs that do not realize the potential of global-local feature extraction.

State Space Model

State Space Model (Kalman 1960), derived from classical control theory, has recently been introduced to deep learning (Gu, Goel, and Ré 2021), (Smith, Warrington, and Linderman 2022), gaining increasing attention. Since the introduction of Mamba (Gu and Dao 2023), a number of efforts have been proposed to leverage its capability for vision applications. Vim (Zhu et al. 2024) introduces a bi-directional SSM scheme that processes tokens in the forward and backward directions to capture global context and improve spatial comprehension. VMamba (Liu et al. 2024) proposes a Cross-Scan module. This module uses a four-way selective scan methodology to integrate information from surrounding tokens and capture the global context. LocalMamba (Huang et al. 2024) has attempted to improve on the scanning direction and to some extent increase the modeling of local 2D dependencies. However, existing visual Mamba architectures still face challenges when dealing with the combination of road surface properties mentioned above for road surface classification due to the lack of effective extraction of local texture.

Methodology

Preliminaries

Structured State Space Models Structured State Space Models (SSMs) provide a principled framework for modeling long-range dependencies in sequential data by introducing a latent state that evolves according to linear dynamics. In continuous time, an SSM is defined by

$$h'(t) = Ah(t) + Bx(t), y(t) = Ch(t) \quad (1)$$

where $x(t) \in \mathbb{R}^L$ is the input sequence, $h(t) \in \mathbb{R}^N$ is the hidden state, $y(t) \in \mathbb{R}^L$ is the output, and $A \in \mathbb{R}^{N \times N}$, $B \in \mathbb{R}^{N \times L}$, $C \in \mathbb{R}^{L \times N}$ govern the system dynamics and readout.

To implement SSMs in discrete-time deep learning frameworks, one commonly applies a zero-order hold (ZOH) discretization over a time step Δ , yielding

$$\bar{A} = e^{\Delta A}, \bar{B} = (\Delta A)^{-1}(e^{\Delta A} - I) \cdot \Delta B \quad (2)$$

so that

$$h_t = \bar{A}h_{t-1} + \bar{B}x_t, y_t = Ch_t \quad (3)$$

Equation 3 can be executed efficiently via associative scans and further recast as a global convolution

$$y = x \circledast \bar{K} \quad (4)$$

$$\bar{K} = (C\bar{B}, C\bar{A}\bar{B}, \dots, C\bar{A}^{L-1}\bar{B})$$

where \circledast denotes convolution and $\bar{K} \in \mathbb{R}^{N \times L}$ is the structured kernel.

Selective State Space Models While classical SSMs (often called S4) scale linearly with sequence length, their use of fixed parameters limits adaptability to varying inputs. Selective State Space Models—exemplified by Mamba—enhance this framework by making the transition and output matrices input-dependent. Specifically, at each time step t , the parameters B_t , C_t , and the discretization Δ_t are generated dynamically from the input x_t , enabling a sequence-aware parameterization that filters out irrelevant information and focuses computation on salient features.

Overall Architecture

Figure 1 illustrates the overall architecture of the RoadMamba model. The model adopts a typical hierarchical design, consisting of a Stem module at the input end for extracting initial low-level features, followed by multiple subsequent stages (Stage 1 to Stage 4) that progressively extract higher-level representations. Within Stages 1 to 4, each stage comprises several DualSSM modules, and the resolution of the feature maps is reduced at the end of each stage via $2\times$ downsampling (Patch Merging) while simultaneously increasing the channel dimension. This process results in a pyramid-like multi-scale feature representation. Such an architecture, similar to most visual models for image classification, captures semantic information at different scales by gradually decreasing spatial resolution through successive layers, while effectively controlling computational costs.

After Stage 4, the network performs multi-scale fusion of the features output by each stage. Specifically, at the end of each stage, we retain the output feature map $F_i \in \mathbb{R}^{H/2^i \times W/2^i \times C_i}$ ($i = 1, 2, 3, 4$), which is then normalized using LayerNorm and aggregated into a channel vector via adaptive average pooling:

$$v_i = \text{GAP}(\text{LayerNorm}(F_i)) \in \mathbb{R}^{C_i} \quad (5)$$

where GAP denotes global average pooling, resulting in a vector of shape $1 \times 1 \times C_i$. The channel vectors from the four stages, v_1, v_2, v_3, v_4 , are concatenated along the channel dimension to obtain the fused multi-scale feature representation:

$$v_{\text{ms}} = [v_1 || v_2 || v_3 || v_4] \in \mathbb{R}^{\sum_{i=1}^4 C_i} \quad (6)$$

where “||” denotes the concatenation operation. This multi-scale feature fusion strategy effectively integrates fine-grained texture, edge information, and deep semantic features extracted at different resolutions, providing richer contextual information for subsequent classification. Finally, the concatenated multi-scale feature vector v_{ms} is fed into the classification head, where a linear layer maps the total channel dimension to the number of classes N_{cls} :

$$\hat{y} = \text{Linear}(v_{\text{ms}}) \in \mathbb{R}^{N_{\text{cls}}} \quad (7)$$

It is worth noting that the entire multi-scale concatenation and classification head are executed only once at the “end” of the model. This design does not alter the computation flow within each stage or increase the intermediate computational load, thus having a negligible impact on the

model’s inference time. Nevertheless, it can significantly improve the final classification performance.

At the heart of RoadMamba lies its customized DualSSM module (which will be detailed in the next subsection), a fundamental unit that integrates both global and local scanning capabilities. Within each DualSSM module, the model extracts global and local features in parallel, and then fuses them through a dual-attention fusion mechanism, enabling the output of each stage to simultaneously capture global contextual information and local details. Residual connections are applied between DualSSM modules. With this design, RoadMamba effectively integrates information while maintaining a deep network and strong representational capacity, thereby providing richer feature representations for downstream tasks.

DualSSM Block

The DualSSM module serves as the fundamental building block of RoadMamba, with its main innovation lying in the integration of both global and local selective state space model (Selective SSM) scanning mechanisms for feature extraction. As illustrated in Figure 2, each DualSSM module contains parallel branches for global scanning and local scanning.

The global scanning branch is responsible for capturing long-range dependencies across the entire feature map. Given an input feature map $X \in \mathbb{R}^{H \times W \times D}$ (where H and W denote the height and width, and D is the number of channels), we flatten the entire feature map along two orthogonal directions into two ultra-long one-dimensional sequences for state space modeling. Specifically, for an input feature tensor \mathbf{X} of shape $H \times W \times D$, we first apply a row-major flattening operation, then a column-major flattening operation is applied to obtain the second sequence.

These two sequences are then fed into one-dimensional SSM units with shared weights. After constant-time stepping and convolutional state updates, we obtain output sequences $\mathbf{y}_h, \mathbf{y}_v \in \mathbb{R}^{(HW) \times D}$. The processed vectors are subsequently reconstructed back into two-dimensional feature maps: specifically, \mathbf{y}_h and \mathbf{y}_v are reshaped into tensors Y_h and Y_v of size $H \times W \times D$, respectively. Finally, these tensors are summed element-wise at each position to produce the global scanning output:

$$Y_{\text{global}} = Y_h + Y_v \quad (8)$$

With this global scanning approach, RoadMamba is able to perceive and model long-range dependencies between any two points in the image within a single forward pass, without being limited by local receptive fields. At the same time, owing to the linear time complexity of SSM, this operation significantly enhances the model’s capacity to capture global context while maintaining high computational efficiency.

The local scanning branch is designed to capture fine-grained local textures and high-frequency details. The input feature map is divided into a grid of non-overlapping windows of size $M \times M$ (with M set to 7 by default), resulting in $n_H \times n_W$ windows, where $n_H = \lceil H/M \rceil$ and $n_W = \lceil W/M \rceil$. For each window block $X_{p,q} \in \mathbb{R}^{M \times M \times D}$

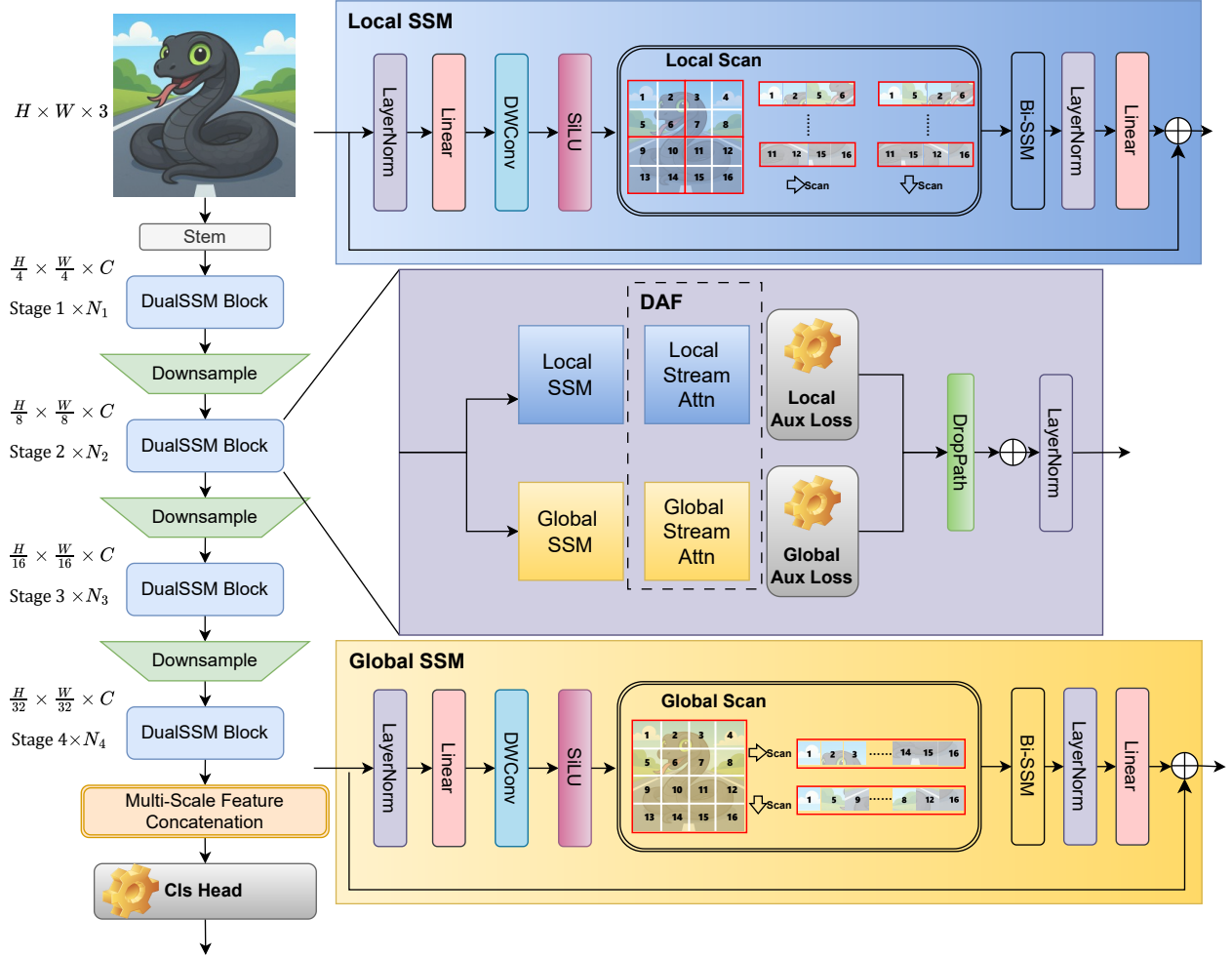


Figure 1: **Architectural details of the RoadMamba.** The model processes the input image through a stem and four stages of DualSSM Blocks, each containing a Local/Global SSM for parallel extraction of global and local features and a Dual Attention Fusion module to enhance extracted local and global features with auxiliary losses. Multi-scale features from all stages are concatenated and fed into the classification head for final prediction.

($0 \leq p < n_H, 0 \leq q < n_W$), we perform both horizontal and vertical SSM scans to obtain the local output $Y_{p,q}^{local}$. However, unlike the global branch, to reduce computational cost, we do not process all windows. Instead, only half of the windows are randomly selected for SSM scanning, while the outputs of the remaining windows are set to zero. Let \mathcal{S} denote the index set of the selected windows, then:

$$Y_{p,q}^{local} = \begin{cases} SSM_h(\cdot) + SSM_v(\cdot) & (p, q) \in \mathcal{S} \\ 0 & (p, q) \notin \mathcal{S} \end{cases} \quad (9)$$

where SSM_h and SSM_v denote the horizontal and vertical SSM transformations applied to each window, respectively. Finally, all local outputs are reassembled to form a feature map $Y_{local} \in \mathbb{R}^{H \times W \times D}$ with the same spatial dimensions as the input. Since only about half of the windows

undergo local scanning, this strategy significantly reduces computational cost and introduces a regularization effect during training similar to Dropout. The incorporation of the local branch enables the model to focus on fine-grained patterns within local regions, thereby complementing the global branch's limited capacity for capturing detailed information.

In the DualSSM module, the global scanning features Y_{global} and the local scanning features Y_{local} are integrated by a subsequent Dual Attention Fusion module (which will be detailed in the next subsection), thereby fully leveraging their complementary information. With this design, each DualSSM module is capable of modeling both global semantics and local textures simultaneously, greatly enhancing the richness and diversity of feature representations.

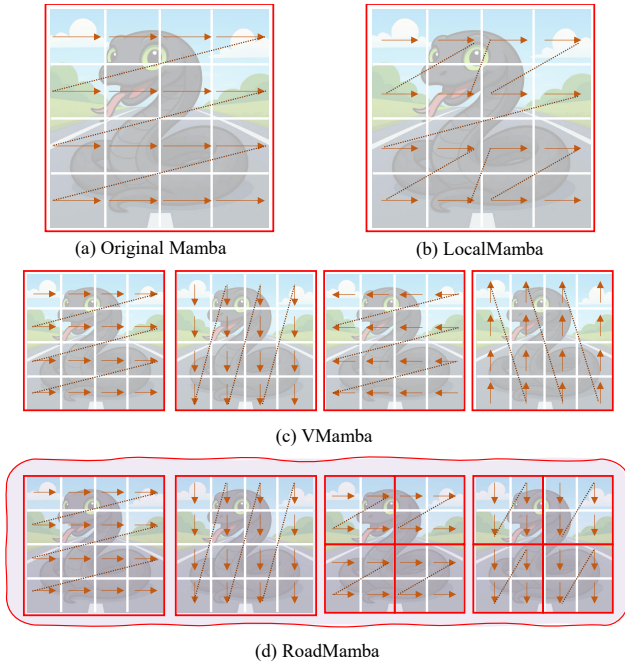


Figure 2: **Illustration of different scanning strategies.** (a) Original Mamba performs global sequential scanning over the entire image. (b) LocalMamba conducts scanning within local windows and serially connects different windows. (c) VMamba extends scanning directions by applying horizontal and vertical scans within windows. (d) The proposed RoadMamba performs bidirectional scanning separately in global and local windows, where each window operates independently. This explicitly differentiates the roles of global and local feature extraction, further enhancing feature representation capability.

Dual Attention Fusion (DAF)

Figure 3 present the structural details of the Dual Attention Fusion (DAF) unit within the DualSSM module. The DAF module is designed to adaptively fuse features extracted from both the global and local branches, thereby fully leveraging the strengths of each. This unit comprises two complementary attention branches: Global Stream Attention and Local Stream Attention, which operate on global and local features, respectively.

For the feature map obtained from global scanning, $Y_{\text{global}} \in \mathbb{R}^{H \times W \times D}$, we apply Global Stream Attention to recalibrate the response intensity of each channel. Specifically, we perform both average pooling and max pooling on Y_{global} along the spatial dimensions. These two channel vectors are then fed into a two-layer MLP and add element by element to produce attention weights for each channel, $\mathbf{w}_c = [w_1, \dots, w_D] = \sigma(W_2(\delta(W_1(\mathbf{u}))))$, where $\delta(\cdot)$ denotes the ReLU activation function, $W_1 \in \mathbb{R}^{D \times D/r}$ and $W_2 \in \mathbb{R}^{D/r \times D}$ are the weight matrices of the two fully connected layers, r is the channel reduction ratio (set to 4 by default), and σ is the sigmoid activation function to ensure the output weights fall within the range of 0 to 1. The

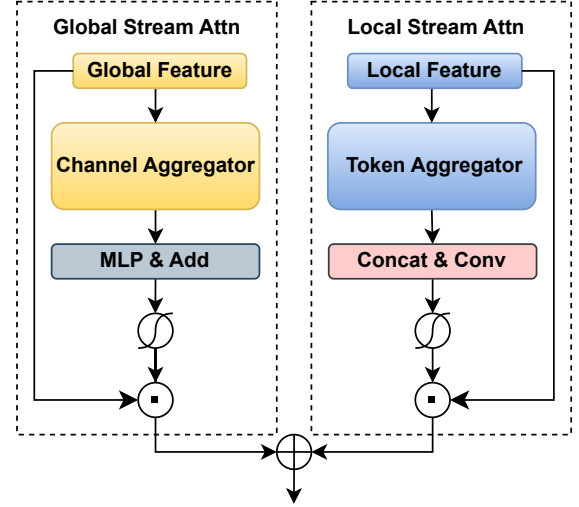


Figure 3: **Illustration of the proposed Dual Attention Fusion.**

resulting channel weights \mathbf{w}_c are multiplied with the original feature map in a channel-wise manner, thus reweighting the channels of the global feature map. The output is the channel-enhanced global feature $Y'_{\text{global}} = \mathbf{w}_c \odot Y_{\text{global}}$.

For the feature map obtained from local scanning, $Y_{\text{local}} \in \mathbb{R}^{H \times W \times D}$, we apply Local Stream Attention to highlight the importance of specific spatial locations. First, we perform both average pooling and max pooling along the channel dimension of Y_{local} , resulting in two single-channel feature maps of size $H \times W$, denoted as M_{avg} and M_{max} . These two maps are then concatenated along the channel dimension to form a two-channel feature map $M_{\text{cat}} \in \mathbb{R}^{2 \times H \times W}$. A 7×7 convolutional layer followed by a sigmoid activation is applied to M_{cat} , producing the spatial attention map $M_s = \sigma(f_{7 \times 7}(M_{\text{cat}})) \in \mathbb{R}^{1 \times H \times W}$. Each element in M_s takes a value between 0 and 1, indicating the importance of the corresponding spatial position. Finally, M_s is broadcast across all D channels and multiplied element-wise with the local features to obtain the spatially enhanced local feature map: $Y'_{\text{local}} = M_s \odot Y_{\text{local}}$.

After computing both channel attention and spatial attention, we sum the enhanced global feature Y'_{global} and the enhanced local feature Y'_{local} element-wise to obtain the fused feature map:

$$Y_{\text{fused}} = Y'_{\text{global}} + Y'_{\text{local}} \quad (10)$$

Subsequently, Y_{fused} is normalized using LayerNorm to produce the final output of the DualSSM module. It is important to emphasize that, unlike simple fusion methods that combine global and local features using fixed weighted summation, the DAF module achieves a more fine-grained and dynamic fusion by applying attention mechanisms along

both the channel and spatial dimensions to global and local information, respectively. This fusion strategy ensures that both global semantics and local details are preserved and enhanced, thereby improving the model’s ability to represent complex visual patterns.

Auxiliary Loss

In the DualSSM module, both the global and local branches are each equipped with an auxiliary classification loss (indicated by gear icons in the figure), implemented via auxiliary classification heads. Each auxiliary head consists of a global average pooling layer followed by a fully connected layer, mapping the corresponding branch’s feature map to an output of the same dimension as the main task. Taking the l -th DualSSM module as an example, let the global branch output be reduced via GAP to $\mathbf{v}_g^{(l)}$, and the local branch output via GAP to $\mathbf{v}_l^{(l)}$. The auxiliary heads produce predictions $\hat{\mathbf{y}}_g^{(l)} = \text{FC}(\mathbf{v}_g^{(l)})$ and $\hat{\mathbf{y}}_l^{(l)} = \text{FC}(\mathbf{v}_l^{(l)})$, respectively. During training, the cross-entropy loss L_{aux} is computed between each auxiliary prediction and the ground-truth label. These auxiliary losses are jointly optimized with the primary loss, and the total loss is defined as:

$$L_{\text{total}} = L_{\text{main}} + \lambda \sum_l \left(L_{\text{aux},g}^{(l)} + L_{\text{aux},l}^{(l)} \right) \quad (11)$$

where L_{main} denotes the loss of the main classification head, while $L_{\text{aux},g}^{(l)}$ and $L_{\text{aux},l}^{(l)}$ represent the auxiliary losses from the global and local heads of the l -th module, respectively. The parameter λ is a balancing coefficient, which is set to $\lambda = 0.3$ in our experiments. It is worth noting that the auxiliary classification heads are used only during the training phase; during inference, these auxiliary branches are removed, introducing no additional computational overhead at test time.

Architecture Variants

We designed several versions of RoadMamba, namely RoadMamba-T, RoadMamba-S, and RoadMamba-B. The parameter counts of these models are comparable to mainstream Mamba-based architectures like VMamba-T, VMamba-S, and VMamba-B. Details of the model configurations can be found in the appendix. The main distinctions among these variants lie in the channel dimensions C and the quantity of blocks within each stage.

Experiments

This section provides an overview of our experimental evaluation. The proposed model was extensively tested on the RSCD dataset and compared in detail with other state-of-the-art models. We also conducted ablation studies to thoroughly assess the contributions of each component in our approach. Furthermore, we discuss the rationale behind adopting a pure Mamba architecture instead of employing window-based attention mechanisms, such as those used in the Swin Transformer, for local feature extraction.

Datasets

The RSCD dataset addresses this shortcoming by providing a large-scale, richly annotated road image dataset, initially comprising 370,000 images and later expanded to one million, covering diverse road materials, usage years, traffic volumes, and a variety of seasonal, weather, and lighting scenarios. RSCD specifically labels road friction (dry, wet, water, fresh snow, melted snow, ice), material type (asphalt, concrete, mud, gravel), and surface unevenness (smooth, slightly uneven, severely uneven), resulting in 27 combined classes. This comprehensive annotation enables more robust research and development in road surface condition recognition for intelligent driving applications.

Evaluation metrics

To evaluate classification performance, we adopt several widely-used metrics, including Top-1 Accuracy, Mean Precision, Mean Recall, and Mean F1 Score. Top-1 Accuracy indicates the percentage of instances where the model’s highest-confidence prediction matches the ground truth, serving as a standard indicator for single-label classification. Precision quantifies the ratio of correctly predicted positive samples to all samples predicted as positive, while Recall measures the proportion of true positives identified among all actual positive cases. These metrics together offer a comprehensive assessment of the model’s classification capability. Given the class imbalance present in the dataset, the F1 Score is also reported as it provides a harmonic mean of Precision and Recall, ensuring a more balanced evaluation.

Implementation Details

All experiments were performed on a single RTX 4090 GPU with a batch size of 32. Model optimization utilized AdamW, following a linear scaling rule to adapt the learning rate to different batch sizes, thus promoting training stability. Additional settings include a weight decay of 0.05, an ε value of 1×10^{-8} for numerical stability, and momentum coefficients $\beta_1 = 0.9$ and $\beta_2 = 0.999$. The learning rate was scheduled using cosine annealing with an initial linear warmup phase.

Comparative Experiments

Our comparative analysis evaluates the performance of the proposed method against several SOTA techniques. These methods include ConvNeXt (Liu et al. 2022), Swin Transformer (Liu et al. 2021), Vision Transformer (Dosovitskiy et al. 2020), VMamba (Liu et al. 2024), MambaVision (Hatamizadeh and Kautz 2025) and LocalMamba (Huang et al. 2024). In Table 1, we present the RSCD classification results. Each model is trained on 40 epochs. Specifically, We compare CNN-based models, Transformer-based models, CNN-Transformer hybrid architecture-based models, and Mamba-based models. Taking the model with the base size as an example, in terms of the Top-1 Accuracy, RoadMamba-B(92.81%) achieves higher accuracy compared to ConvNeXt-B(84.08%), Swin-B(85.68%), ViT-B(86.83%), VMamba-B(91.11%) and MambaVision-B(92.07%). Under the remaining three evaluation metrics,

Table 1: Comparison Experiments between RoadMamba and other SOTA models.

Model	Top-1 Acc	Mean-P	Mean-R	Mean-F1	Params	GFLOPs
ConvNeXt-T	82.27	73.35	68.35	70.27	29M	4.5
ConvNeXt-S	84.08	76.35	70.24	72.59	50M	8.7
ConvNeXt-B	84.08	75.55	70.50	72.48	89M	15.4
ConvNeXt-L	84.88	76.65	72.36	74.20	198M	34.4
Swin-T	85.39	77.52	72.52	74.55	28M	4.5
Swin-S	85.16	77.21	72.44	74.44	50M	8.7
Swin-B	85.68	77.69	73.24	75.08	88M	15.4
Swin-L	87.38	80.47	76.03	77.91	197M	34.4
ViT-B	86.83	78.31	74.99	76.38	86M	18.5
ViT-L	88.47	79.99	77.51	78.58	307M	63.3
VMamba-T	90.79	83.12	79.45	81.04	30M	4.9
VMamba-S	90.66	83.07	79.28	80.90	50M	8.7
VMamba-B	91.11	83.52	80.11	81.60	89M	15.4
LocalMamba-T	91.68	84.41	81.14	82.58	26M	9.7
LocalMamba-S	92.05	84.62	81.23	82.63	50M	11.0
MambaVision-T	91.52	84.10	80.77	82.23	32M	4.4
MambaVision-S	91.55	84.18	81.48	82.67	50M	7.5
MambaVision-B	92.07	84.99	82.23	83.49	98M	15.0
MambaVision-L	92.40	85.38	82.51	83.82	227M	34.9
RoadMamba-T	92.58	85.84	83.05	84.31	28M	5.1
RoadMamba-S	92.63	85.84	83.42	84.53	43M	8.7
RoadMamba-B	92.81	85.92	83.73	84.79	86M	15.8

Table 2: Performance comparison between Swin Transformer and WindowMamba.

Model	Top-1 Acc	Mean-P	Mean-R	Mean-F1
Swin-T	85.39	77.52	72.52	74.55
WindowMamba-T	89.22	80.08	75.46	77.31

our approach also surpasses the others. This indicates that the RoadMamba proposed by us is an effective and promising paradigm.

Why Choose Mamba?

In designing our global-local dual-stream Mamba framework, a natural consideration was whether to incorporate window-based attention mechanisms, which have achieved remarkable success in architectures such as Swin Transformer. To rigorously justify our choice of adopting a pure Mamba architecture instead of integrating window-based attention, we conducted controlled comparative experiments. Specifically, we evaluated the performance of a window-based variant of Mamba (WindowMamba), using an identical window size as in Swin Transformer, and compared its performance directly against Swin Transformer.

In Table2 experimental results clearly demonstrated the

Table 3: Ablation Experiment, A represents the dual scanning strategy, B represents DAF, C represents Auxiliary Loss.

Model	Top-1 Acc	Mean-P	Mean-R	Mean-F1
Without A&B&C	90.46	82.59	78.65	80.35
Without B&C	90.62	82.71	79.30	80.81
Without C	91.35	83.86	80.40	81.91
RoadMamba	91.52	84.35	80.95	82.44

superiority of WindowMamba over Swin Transformer, achieving notably higher accuracy metrics on the same dataset and task settings.

Consequently, our findings reinforce the choice of a purely Mamba-based approach. The improved accuracy coupled with reduced computational complexity underscores Mamba’s advantage as a robust alternative to attention-based mechanisms, thus aligning with our goal of developing an efficient yet powerful model for fine-grained classification tasks.

Ablation Study

In this section, we present a set of ablation experiments to verify the effectiveness of the dual scanning strategy, DAF and auxiliary loss. Each model is trained on 20 epochs. More ablation experiments are presented in the appendix.

As shown in Table3, to thoroughly investigate the contribution of each proposed component within our architecture, we conducted comprehensive ablation experiments. Specifically, we evaluated the individual impacts of the dual scanning strategy, DAF and Auxiliary Loss on the model’s overall performance.

We first evaluated the baseline model that excluded all three proposed modules, corresponding to a Mamba architecture with only global scanning. Introducing the dual scanning mechanism resulted in a 0.16% improvement in Top-1 accuracy. Further incorporating the Dual Attention Fusion led to an additional 0.73% increase. Finally, adding the auxiliary loss yielded a further 0.17% gain in Top-1 accuracy.

Overall, the ablation studies demonstrate the individual and collective importance of each component in our proposed framework, confirming their essential roles in achieving superior fine-grained classification performance.

Conclusion

In summary, this work pioneers the application of visual Mamba-based architectures to the field of road surface classification. We introduced RoadMamba, a novel framework that seamlessly integrates both local and global feature perception through the Dual State Space Model (DualSSM) and an effective Dual Attention Fusion (DAF) mechanism. By explicitly incorporating an auxiliary loss, our approach ensures balanced learning in the dual branches, mitigating the risk of over-reliance on global semantic cues and promoting the retention of critical local texture information. Extensive experiments conducted on RSCD dataset with one million

road surface images demonstrate that RoadMamba sets a new benchmark for performance in this domain, confirming the potential of Mamba architectures for fine-grained scene understanding tasks.

References

- Caesar, H.; Bankiti, V.; Lang, A. H.; Vora, S.; Liong, V. E.; Xu, Q.; Krishnan, A.; Pan, Y.; Baldan, G.; and Beijbom, O. 2020. nuscenes: A multimodal dataset for autonomous driving. In *Proceedings of the IEEE/CVF conference on computer vision and pattern recognition*, 11621–11631.
- Chen, Y.; Qin, H.; Zhang, Z.; Magno, M.; Benini, L.; and Li, Y. 2025. Q-mambair: Accurate quantized mamba for efficient image restoration. *arXiv preprint arXiv:2503.21970*.
- Dhiman, A.; and Klette, R. 2019. Pothole detection using computer vision and learning. *IEEE Transactions on Intelligent Transportation Systems*, 21(8): 3536–3550.
- Dosovitskiy, A.; Beyer, L.; Kolesnikov, A.; Weissenborn, D.; Zhai, X.; Unterthiner, T.; Dehghani, M.; Minderer, M.; Heigold, G.; Gelly, S.; et al. 2020. An image is worth 16x16 words: Transformers for image recognition at scale. *arXiv preprint arXiv:2010.11929*.
- Geiger, A.; Lenz, P.; Stiller, C.; and Urtasun, R. 2013. Vision meets robotics: The kitti dataset. *The international journal of robotics research*, 32(11): 1231–1237.
- Gu, A.; and Dao, T. 2023. Mamba: Linear-time sequence modeling with selective state spaces. *arXiv preprint arXiv:2312.00752*.
- Gu, A.; Goel, K.; and Ré, C. 2021. Efficiently modeling long sequences with structured state spaces. *arXiv preprint arXiv:2111.00396*.
- Guo, H.; Li, J.; Dai, T.; Ouyang, Z.; Ren, X.; and Xia, S.-T. 2024. Mambair: A simple baseline for image restoration with state-space model. In *European conference on computer vision*, 222–241. Springer.
- Hatamizadeh, A.; and Kautz, J. 2025. Mambavision: A hybrid mamba-transformer vision backbone. In *Proceedings of the Computer Vision and Pattern Recognition Conference*, 25261–25270.
- Huang, T.; Pei, X.; You, S.; Wang, F.; Qian, C.; and Xu, C. 2024. Localmamba: Visual state space model with windowed selective scan. In *European Conference on Computer Vision*, 12–22. Springer.
- Kalman, R. E. 1960. A new approach to linear filtering and prediction problems.
- Leng, B.; Jin, D.; Xiong, L.; Yang, X.; and Yu, Z. 2021. Estimation of tire-road peak adhesion coefficient for intelligent electric vehicles based on camera and tire dynamics information fusion. *Mechanical Systems and Signal Processing*, 150: 107275.
- Liu, Y.; Tian, Y.; Zhao, Y.; Yu, H.; Xie, L.; Wang, Y.; Ye, Q.; Jiao, J.; and Liu, Y. 2024. Vmamba: Visual state space model. *Advances in neural information processing systems*, 37: 103031–103063.
- Liu, Z.; Lin, Y.; Cao, Y.; Hu, H.; Wei, Y.; Zhang, Z.; Lin, S.; and Guo, B. 2021. Swin transformer: Hierarchical vision transformer using shifted windows. In *Proceedings of the IEEE/CVF international conference on computer vision*, 10012–10022.
- Liu, Z.; Mao, H.; Wu, C.-Y.; Feichtenhofer, C.; Darrell, T.; and Xie, S. 2022. A convnet for the 2020s. In *Proceedings of the IEEE/CVF conference on computer vision and pattern recognition*, 11976–11986.
- Nolte, M.; Kister, N.; and Maurer, M. 2018. Assessment of deep convolutional neural networks for road surface classification. In *2018 21st International Conference on Intelligent Transportation Systems (ITSC)*, 381–386. IEEE.
- Roychowdhury, S.; Zhao, M.; Wallin, A.; Ohlsson, N.; and Jonasson, M. 2018. Machine learning models for road surface and friction estimation using front-camera images. In *2018 International Joint Conference on Neural Networks (IJCNN)*, 1–8. IEEE.
- Šabanovič, E.; Žuraulis, V.; Prentkovskis, O.; and Skrickij, V. 2020. Identification of road-surface type using deep neural networks for friction coefficient estimation. *Sensors*, 20(3): 612.
- Smith, J. T.; Warrington, A.; and Linderman, S. W. 2022. Simplified state space layers for sequence modeling. *arXiv preprint arXiv:2208.04933*.
- Sun, P.; Kretschmar, H.; Dotiwalla, X.; Chouard, A.; Patnaik, V.; Tsui, P.; Guo, J.; Zhou, Y.; Chai, Y.; Caine, B.; et al. 2020. Scalability in perception for autonomous driving: Waymo open dataset. In *Proceedings of the IEEE/CVF conference on computer vision and pattern recognition*, 2446–2454.
- Tian, C.; Jin, D.; Leng, B.; and Xiong, L. 2021. Reliable identification of road surface condition considering shadow interference. In *2021 IEEE International Intelligent Transportation Systems Conference (ITSC)*, 251–257. IEEE.
- Wang, T.; Zhang, Z.; and Sun, C. 2025. RoadFormer: Local-Global Feature Fusion for Road Surface Classification in Autonomous Driving. *arXiv preprint arXiv:2506.02358*.
- Yang, L.; Yu, K.; Tang, T.; Li, J.; Yuan, K.; Wang, L.; Zhang, X.; and Chen, P. 2023. Bevheight: A robust framework for vision-based roadside 3d object detection. In *Proceedings of the IEEE/CVF Conference on Computer Vision and Pattern Recognition*, 21611–21620.
- Yu, H.; Luo, Y.; Shu, M.; Huo, Y.; Yang, Z.; Shi, Y.; Guo, Z.; Li, H.; Hu, X.; Yuan, J.; et al. 2022. Dair-v2x: A large-scale dataset for vehicle-infrastructure cooperative 3d object detection. In *Proceedings of the IEEE/CVF conference on computer vision and pattern recognition*, 21361–21370.
- Zhang, Z.; Sun, C.; Wang, B.; Guo, B.; Wen, D.; Zhu, T.; and Ning, Q. 2025a. Height3d: A roadside visual framework based on height prediction in real 3-d space. *IEEE Transactions on Intelligent Transportation Systems*.
- Zhang, Z.; Sun, C.; Yue, C.; Wen, D.; Chen, Y.; Wang, T.; and Leng, J. 2025b. Heightformer: Learning height prediction in voxel features for roadside vision centric 3d object detection via transformer. *arXiv preprint arXiv:2503.10777*.

Zhang, Z.; Sun, C.; Yue, C.; Wen, D.; Wang, T.; and Leng, J. 2025c. Pillarmamba: Learning local-global context for roadside point cloud via hybrid state space model. *arXiv preprint arXiv:2505.05397*.

Zhao, T.; He, J.; Lv, J.; Min, D.; and Wei, Y. 2023. A comprehensive implementation of road surface classification for vehicle driving assistance: Dataset, models, and deployment. *IEEE Transactions on Intelligent Transportation Systems*, 24(8): 8361–8370.

Zhu, L.; Liao, B.; Zhang, Q.; Wang, X.; Liu, W.; and Wang, X. 2024. Vision mamba: Efficient visual representation learning with bidirectional state space model. *arXiv preprint arXiv:2401.09417*.

Appendix

Supplemental Ablation Experiments

Ablation Study on Scanning Strategies Table4 presents the results of the supplemental ablation experiment comparing the performance of models employing only global scanning (GlobalMamba), only local scanning (WindowMamba), and the proposed dual-stream strategy (RoadMamba*). * represents that in this set of ablation experiments, Roadmamba only has a different scanning method from the previous two, and there is no increase in DAF module and auxiliary loss. As shown, RoadMamba consistently achieves the highest scores across all evaluation metrics, including Top-1 Accuracy, Mean Precision, Mean Recall, and Mean F1 Score. In contrast, both GlobalMamba and WindowMamba yield inferior results, indicating that relying solely on either global or local scan strategies limits the model’s capacity for comprehensive feature extraction. These findings clearly demonstrate the effectiveness of RoadMamba’s integration of both global and local scanning mechanisms, which enables more robust and accurate road surface classification.

Ablation Study on Aggregator Assignment for Global and Local Streams Table5 reports the results of the supplemental ablation experiment investigating different pathways for aggregating global and local features. Specifically, the results compare three configurations: GLTC (both global and local features pass through the Channel Aggregator and Token Aggregator), GTLC (global features use the Token Aggregator while local features use the Channel Aggregator), and GCLT (global features use the Channel Aggregator while local features use the Token Aggregator, i.e., the

Table 4: Supplemental Ablation Experiment A, GlobalMamba represents the strategy only uses Global Scan, WindowMamba represents the strategy only uses Local Scan.

Model	Top-1 Acc	Mean-P	Mean-R	Mean-F1
GlobalMamba	90.46	82.59	78.65	80.35
WindowMamba	89.22	80.08	75.46	77.31
RoadMamba*	90.62	82.71	79.30	80.81

Table 5: Supplemental Ablation Experiment B, GLTC represents both global and local features go through the Channel Aggregator and Token Aggregator, GTLC represents global feature goes through the Token Aggregator and local feature goes through the Channel Aggregator, GCLT represents global feature goes through the Channel Aggregator and local feature goes through the Token Aggregator.

Model	Top-1 Acc	Mean-P	Mean-R	Mean-F1
GLTC	91.29	83.85	80.35	81.87
GTLC	91.12	83.49	80.08	81.59
GCLT	91.35	83.86	80.40	81.91

RoadMamba design). Among the three, the GCLT configuration achieves the best performance across all evaluation metrics, including Top-1 Accuracy, Mean Precision, Mean Recall, and Mean F1 Score. This demonstrates that assigning the Channel Aggregator to the global stream and the Token Aggregator to the local stream is the most effective strategy, highlighting the critical role of this architectural design in enabling RoadMamba to achieve superior road surface classification results.

Table 6: Architectural overview of the RoadMamba series.

layer name	output size	RoadMamba-T	RoadMamba-S	RoadMamba-B
stem	112×112	conv 4×4 , 96, stride 4	conv 4×4 , 96, stride 4	conv 4×4 , 128, stride 4
stage 1	56×56	DualSSM Block $\left[\begin{array}{l} \text{Linear } 96 \rightarrow 384 \\ \text{DWConv } 3 \times 3, 192 \\ \text{SS2D(Global Scan), } 192 \\ \text{SS2D(Local Scan), } 192 \\ \text{Multiplicative} \\ \text{Linear } 192 \rightarrow 96 \end{array} \right] \times 1$ patch merging $\rightarrow 192$	DualSSM Block $\left[\begin{array}{l} \text{Linear } 96 \rightarrow 384 \\ \text{DWConv } 3 \times 3, 192 \\ \text{SS2D(Global Scan), } 192 \\ \text{SS2D(Local Scan), } 192 \\ \text{Multiplicative} \\ \text{Linear } 192 \rightarrow 96 \end{array} \right] \times 3$ patch merging $\rightarrow 192$	DualSSM Block $\left[\begin{array}{l} \text{Linear } 128 \rightarrow 512 \\ \text{DWConv } 3 \times 3, 256 \\ \text{SS2D(Global Scan), } 256 \\ \text{SS2D(Local Scan), } 256 \\ \text{Multiplicative} \\ \text{Linear } 256 \rightarrow 128 \end{array} \right] \times 3$ patch merging $\rightarrow 256$
stage 2	28×28	DualSSM Block $\left[\begin{array}{l} \text{Linear } 192 \rightarrow 768 \\ \text{DWConv } 3 \times 3, 384 \\ \text{SS2D(Global Scan), } 384 \\ \text{SS2D(Local Scan), } 384 \\ \text{Multiplicative} \\ \text{Linear } 384 \rightarrow 192 \end{array} \right] \times 3$ patch merging $\rightarrow 384$	DualSSM Block $\left[\begin{array}{l} \text{Linear } 192 \rightarrow 768 \\ \text{DWConv } 3 \times 3, 384 \\ \text{SS2D(Global Scan), } 384 \\ \text{SS2D(Local Scan), } 384 \\ \text{Multiplicative} \\ \text{Linear } 384 \rightarrow 192 \end{array} \right] \times 3$ patch merging $\rightarrow 384$	DualSSM Block $\left[\begin{array}{l} \text{Linear } 256 \rightarrow 1024 \\ \text{DWConv } 3 \times 3, 512 \\ \text{SS2D(Global Scan), } 512 \\ \text{SS2D(Local Scan), } 512 \\ \text{Multiplicative} \\ \text{Linear } 512 \rightarrow 256 \end{array} \right] \times 3$ patch merging $\rightarrow 512$
stage 3	14×14	DualSSM Block $\left[\begin{array}{l} \text{Linear } 384 \rightarrow 1536 \\ \text{DWConv } 3 \times 3, 768 \\ \text{SS2D(Global Scan), } 768 \\ \text{SS2D(Local Scan), } 768 \\ \text{Multiplicative} \\ \text{Linear } 768 \rightarrow 384 \end{array} \right] \times 6$ patch merging $\rightarrow 768$	DualSSM Block $\left[\begin{array}{l} \text{Linear } 384 \rightarrow 1536 \\ \text{DWConv } 3 \times 3, 768 \\ \text{SS2D(Global Scan), } 768 \\ \text{SS2D(Local Scan), } 768 \\ \text{Multiplicative} \\ \text{Linear } 768 \rightarrow 384 \end{array} \right] \times 10$ patch merging $\rightarrow 768$	DualSSM Block $\left[\begin{array}{l} \text{Linear } 512 \rightarrow 2048 \\ \text{DWConv } 3 \times 3, 1024 \\ \text{SS2D(Global Scan), } 1024 \\ \text{SS2D(Local Scan), } 1024 \\ \text{Multiplicative} \\ \text{Linear } 1024 \rightarrow 512 \end{array} \right] \times 15$ patch merging $\rightarrow 1024$
stage 4	7×7	DualSSM Block $\left[\begin{array}{l} \text{Linear } 768 \rightarrow 3072 \\ \text{DWConv } 3 \times 3, 1536 \\ \text{SS2D(Global Scan), } 1536 \\ \text{SS2D(Local Scan), } 1536 \\ \text{Multiplicative} \\ \text{Linear } 1536 \rightarrow 768 \end{array} \right] \times 3$	DualSSM Block $\left[\begin{array}{l} \text{Linear } 768 \rightarrow 3072 \\ \text{DWConv } 3 \times 3, 1536 \\ \text{SS2D(Global Scan), } 1536 \\ \text{SS2D(Local Scan), } 1536 \\ \text{Multiplicative} \\ \text{Linear } 1536 \rightarrow 768 \end{array} \right] \times 3$	DualSSM Block $\left[\begin{array}{l} \text{Linear } 1024 \rightarrow 4096 \\ \text{DWConv } 3 \times 3, 2048 \\ \text{SS2D(Global Scan), } 2048 \\ \text{SS2D(Local Scan), } 2048 \\ \text{Multiplicative} \\ \text{Linear } 2048 \rightarrow 1024 \end{array} \right] \times 3$
average pool, 27-d fc, softmax				
Param. (M)		28	46	86
FLOPs		5.1×10^9	8.7×10^9	15.8×10^9